

# Supplementary materials: Infiltration of CD8<sup>+</sup> T cells into tumor-cell clusters in Triple Negative Breast Cancer

Xuefei Li<sup>\*1</sup>, Tina Gruosso<sup>\*2,3</sup>, Dongmei Zuo<sup>2</sup>, Atilla Omeroglu<sup>4</sup>, Sarkis Meterissian<sup>3,5</sup>, Marie-Christine Guiot<sup>4,6</sup>, Adam Salazar<sup>1</sup>, Morag Park<sup>†2,3,7</sup>,  
and Herbert Levine<sup>‡1,8,9</sup>

<sup>1</sup>Center for Theoretical Biological Physics, Rice University, Houston, TX  
77030

<sup>2</sup>Goodman Cancer Research Centre, McGill University, Montreal, QC H3A  
1A3, Canada

<sup>3</sup>Department of Oncology, McGill University, Montreal, QC H4A 3T2,  
Canada

<sup>4</sup>Department of Pathology, McGill University Health Centre, Montreal, QC  
H4A 3J1, Canada

<sup>5</sup>Department of Surgery, McGill University Health Centre, Montreal H4A  
3J1, QC, Canada

<sup>6</sup>Montreal Neurological Institute and Hospital, McGill University, Montreal,  
QC H3A 2B4, Canada

<sup>7</sup>Department of Biochemistry, McGill University, Montreal, QC H3A 1A3,  
Canada

<sup>8</sup>Department of Bioengineering, Rice University, Houston, TX 77030

<sup>9</sup>Department of Physics, Northeastern University, Boston, MA 02115

January 24, 2019

---

\*These authors contributed equally

†morag.park@mcgill.ca

‡herbert.levine@rice.edu

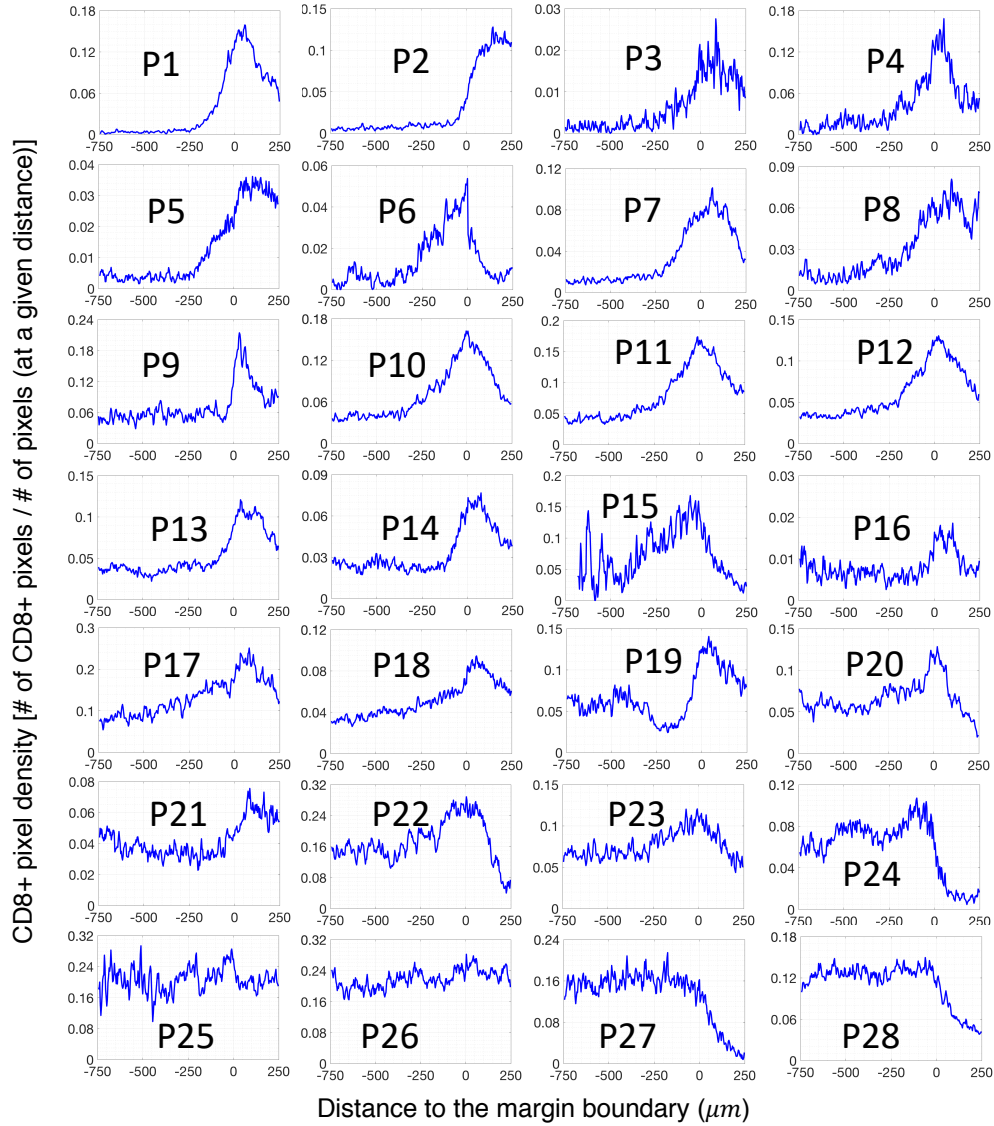


Fig. S1: Spatial profiles of CD8<sup>+</sup>-pixel density across the tumor-margin boundary for all 28 patients. We focused on the region between  $-750\mu m$  and  $250\mu m$  around the margin boundary. The negative distance corresponds to the region inside of the margin boundary and vice versa. The patient number is assigned according to the level of T-cell infiltration across tumor-margin boundary. In addition, there is a characteristic accumulation of T cells in the region between  $-250\mu m$  and  $250\mu m$  for most patients (P1-P26).

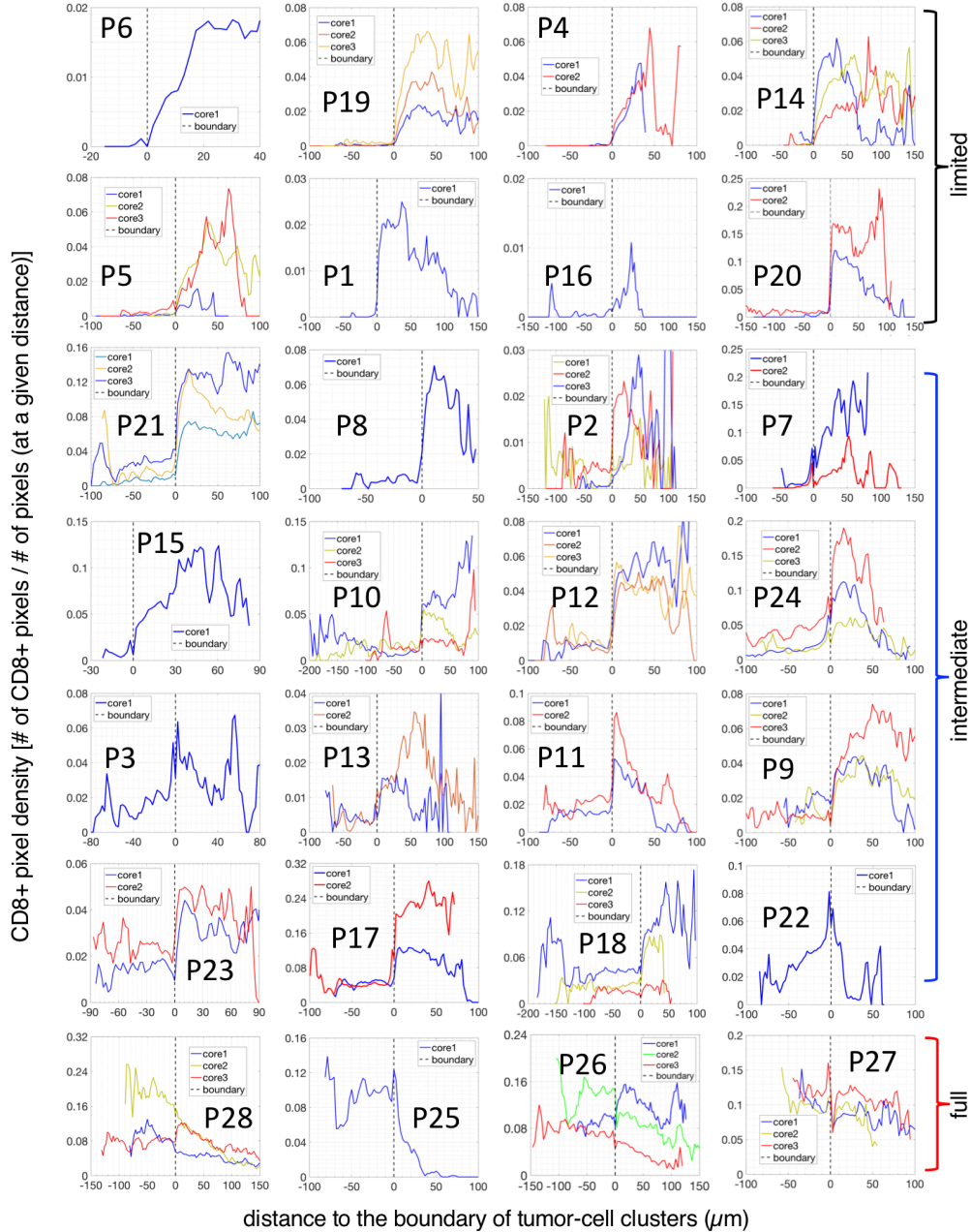


Fig. S2: Spatial profiles of the CD8<sup>+</sup>-density across the boundary of tumor-cell clusters for all 28 patients. The negative distance corresponds to the region inside of tumor-cell clusters and the positive distance corresponds to the stroma region in the tumor core. The level of T-cell infiltration into tumor-cell clusters increases from left to right and from top to bottom. The 8 patients in the top two rows are characterized as the ones with limited CD8<sup>+</sup> T-cell infiltration; the 4 patients at the bottom row are characterized as the ones with full infiltration; other patients have the intermediate CD8<sup>+</sup> T-cell infiltration. For each tumor, as many as 3 regions in the tumor core were selected and analyzed. The quantified profile for each core region is shown in a blue, red, or green line. For patients with intermediate infiltrations, in many regions (e.g., P2, P13, P21-core2, etc.), the CD8<sup>+</sup> T cell density first decreases when moving from the boundary to the center of the tumor-cell clusters and then rises again when approaching the center.

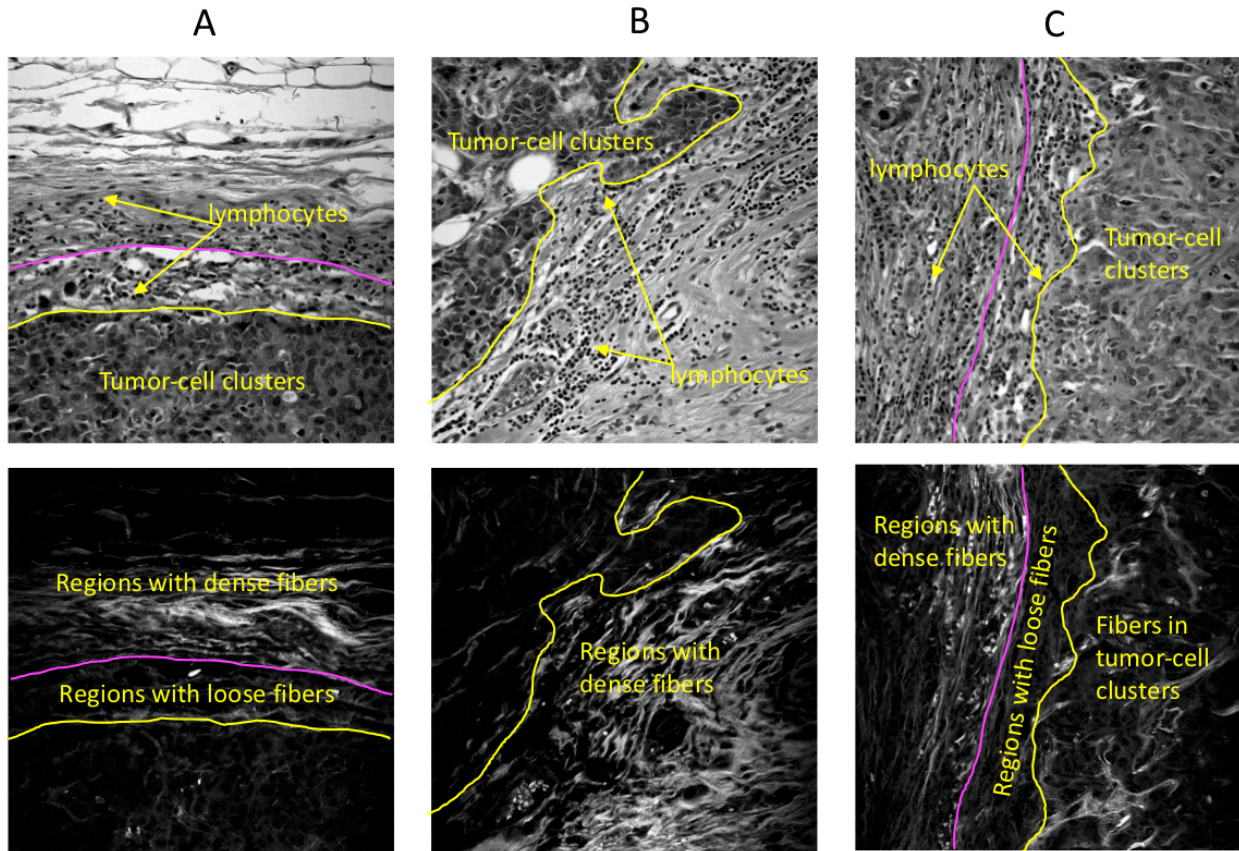


Fig. S3: Representative invasive margins of three tumors are presented. Top row: phase contrast image of selected margins. Bottom row: Second-Harmonic Generation (SHG) images of the corresponding regions, which shows the pattern of collagen fibers (bright area). These examples show that lymphocytes can accumulate in regions close to the boundary of tumor-cell clusters instead of being constrained in regions with dense fibers. Representative lymphocytes are indicated by yellow arrows. Margins of the tumors are marked by yellow lines and the boundary between dense- and loose-fiber regions is manually marked by cyan lines.



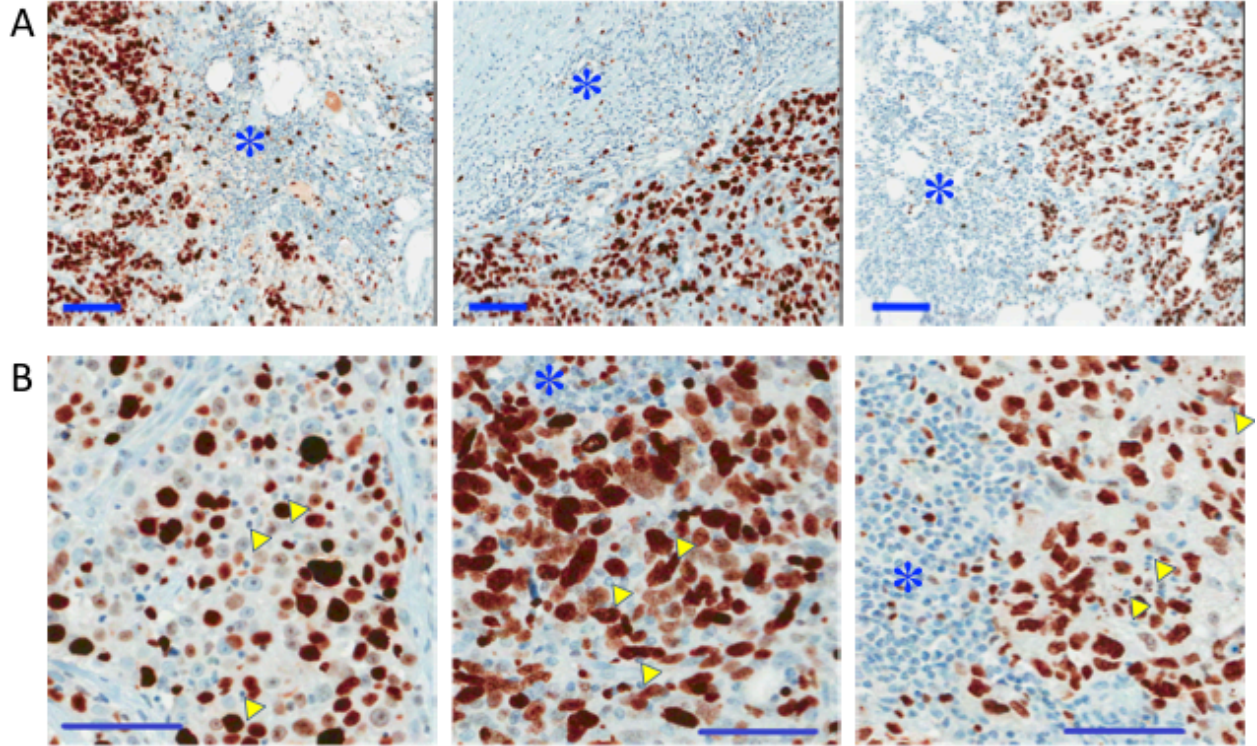


Fig. S4: Examples of patient specimens with ki67 staining. A. These three examples are from the patient group with limited infiltration of CD8<sup>+</sup> T lymphocytes, i.e., CD8<sup>+</sup> cells are mostly outside of tumor-cell clusters. The three examples are from three different patients. In stroma (areas indicated with blue stars), most lymphocytes, characterized by small and round nucleus, are not ki67<sup>+</sup>. B. These three examples are from the patient group with full infiltration of CD8<sup>+</sup> T lymphocytes, i.e., CD8<sup>+</sup> cells density inside of tumor-cell clusters is higher than that outside. The three examples are from three different patients. Again, similar to the case in A, in stroma (areas indicated with blue stars), most lymphocytes are not ki67<sup>+</sup>. Furthermore, inside of tumor-cell clusters, many lymphocytes are not ki67<sup>+</sup>. Three lymphocytes are selected for each images for illustration, marked by yellow arrowheads. Scale bars: 100 $\mu$ m.

### Fitting the CD8<sup>+</sup> spatial profiles with the repellent model

In order to demonstrate the possibility of explaining the CD8<sup>+</sup> spatial profiles with our repellent model, we show in Fig S5 a few examples of data fit by our model with several patient-specific parameter values. In Fig. S5. In all these fits, we re-scaled the simulation region according to the actual scale and the diffusion coefficient of T cells was always taken to equal a realistic value of 5 $\mu$ m<sup>2</sup>/min. Also, the diffusion coefficients of the attractant and repellent were uniformly set to 600 $\mu$ m<sup>2</sup>/min. The production and degradation rates of chemo-attractant are constants, except for the example in Fig. S5F. The degradation rate of chemo-repellent is constant and the chemotaxis coefficients are also kept as constants. The first key parameter tuned in different examples is the production rate for chemo-repellent. Secondly, the region over which tumor cells secrete chemo-repellent is also tuned, especially for the case with intermediate-infiltration. In addition, the initial number of T cells is also

tuned to match the density to the measured value.

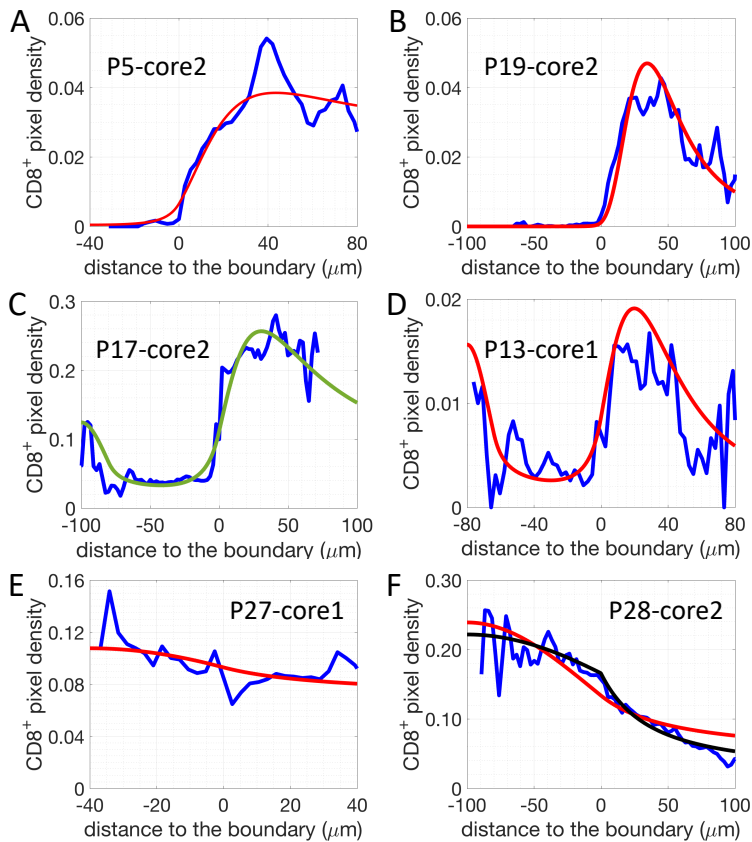


Fig. S5: Examples of fitting data with the chemo-repellent model. A and B. Two examples of limited-infiltration tumors. The fitting parameters for A: the production rate of chemo-repellent ( $\alpha_R$ ) is 70; the initial T density equals to 1 between  $r = 3$  and  $r = 3.25$ ; the simulated region is between  $r = 0$  and  $r = 6$ . For B, the parameters are  $\alpha_R = 120$ , the initial T density equals to 1 between  $r = 3$  and  $r = 3.05$ . For both A and B, the simulated region is between  $r = 0$  and  $r = 4$  and the repellent is assumed to be expressed by all tumor cells. C and D. Two examples of intermediate-infiltration tumors. For C, the fitting parameters are  $\alpha_R = 31$ , the initial T density equals to 1 between  $r = 3$  and  $r = 3.38$ , and the production rate of chemo-attractant ( $\alpha_A$ ) equals to 0.3 (in A and B,  $\alpha_A = 1$ ). For D, the fitting parameters are  $\alpha_R = 55$ , the initial T density equals to 1 between  $r = 3$  and  $r = 3.03$ , and  $\alpha_A = 1$ . For both C and D, the simulated region is between  $r = 0$  and  $r = 4$  and the repellent is assumed to be expressed by tumor cells in the region between  $r = 0.4$  and  $r = 2$ . E and F. Two examples of full-infiltration tumors. For E,  $\alpha_A = 0.15$ , the initial T density equals to 1 between  $r = 3$  and  $r = 3.19$ . For the red fitting line in F, the initial T density equals to 1 between  $r = 3$  and  $r = 3.22$  and  $\alpha_A = 0.1$ . For the black fitting line in F, the initial T density equals to 1 between  $r = 3$  and  $r = 3.2$  and  $\alpha_A = 0.05$ . For both E and F,  $\alpha_R = 0$  and the simulated region is between  $r = 0$  and  $r = 4$ . Note that the boundary is at  $r = 2$  in all models.  $r = 1$  corresponds to  $20\mu m$ ,  $50\mu m$ ,  $50\mu m$ ,  $40\mu m$ ,  $20\mu m$ , and  $50\mu m$  in A, B, C, D, E, and F, respectively. For all cases, chemotaxis coefficient for the repellent ( $\lambda_R$ ) and attractant ( $\lambda_A$ ) are the same for all cases, which correspond to  $200\mu m^2/mM/h$  and  $2000\mu m^2/mM/h$ , respectively.

**Preliminary efforts made to identify chemokines enriched in tumors with limited-**

## infiltration of CD8<sup>+</sup> T cells

In order to see if it is currently possible to identify candidates for the hypothetical repellent of CD8<sup>+</sup> T cells, we selected several patients out of the 28 patients and binned them into two groups according to the level of CD8<sup>+</sup> T-cell infiltration. Specifically, we selected 5 patients with limited infiltration on the tumor-cell cluster level (P6, P19, P4, P14, P5) and another 5 patients with high infiltration (P22, P25, P26, P27, P28). Among the 19700 genes measured (bulk tumor gene expression data, GSE58644), we focused on the chemokines that have a higher expression in the 5 tumors with limited infiltrations. Out of 39 chemokines investigated, CCL28 has the biggest positive fold change (1.2-fold, limited/high infiltration) and lowest p-value (0.064). The corresponding q-value is 0.84, which is very high and indicate that CCL28 might be characterized as a false-positive case. As a consistency check, CXCL9, a T-cell attractant, has the biggest negative fold change (-1.2 fold, limited/high infiltration) and lowest p-value (0.0008). The corresponding q-value is 0.4, which is also high.

We then selected 10 patients (5 per each group) by considering the infiltration both on the tumor-cell cluster level and the tumor-margin level. The 5 patients with lower infiltrations are P1, P2, P4, P5, P6, and P7; the 5 patients with higher infiltrations are P23, P25, P26, P27, P28. For these two groups of patients, out of 39 chemokines investigated, CCL28 also has the highest fold change (1.3-fold, limited/high infiltration) and lowest p-value (0.003). The corresponding q-value is 0.72, which is again very high and again indicates that CCL28 might be characterized as a false-positive case. As a consistency check, CXCL9 has the biggest negative fold change (-1.16 fold, limited/high infiltration) and lowest p-value (0.007). The corresponding q-value is 0.78, which is also high.

Since the fold change tested was not very significant, we set out to test the correlations between infiltration levels (characterized in this work) and the expression level of each gene. Again, we found a negative correlation between the gene expression of *ccl28* and the infiltration level on both tumor-cell cluster level (correlation coefficient: -0.31, p-value: 0.11, q-value: 0.89) and tumor-margin level (correlation coefficient: -0.31, p-value: 0.1, q-value: 0.98). The correlation coefficients rank the lowest (negative) of 39 chemokines investigated. But the statistics were not significant. As a positive control, the corresponding coefficients for CCL5, the highest-ranked T-cell attractant in this analysis, are 0.53 (p-value: 0.004, q-value: 0.42) and 0.63 (p-value: 0.0003, q-value: 0.39), respectively.

In summary, our analysis on the gene expression data of bulk tumors did not reveal a statistically-significant candidate of the repellent. However, this might be because reason that we do at present cannot investigate the gene expression data of pure cancer cells. Nonetheless, the current analysis suggests that *ccl28* might be a promising candidate to be investigated further.